Subduction Initiation and Ophiolite Crust: New Insights From IODP Drilling

Mark K. Reagan*, *Department of Earth & Environmental Sciences, University of Iowa, Iowa City IA 52242, USA, mark-reagan@uiowa.edu.*
Julian A. Pearce, *School of Earth & Ocean Sciences, Cardiff University, Cardiff CF10 3AT, United Kingdom.*
Katerina Petronotis, *International Ocean Discovery Program, Texas A&M University, College Station TX 77845-9547 USA.*
Renat R. Almeev, *Institüt für Mineralogie, Leibniz Universität Hannover 30167, Hannover Germany.*
Aaron J. Avery, *Earth, Ocean and Atmospheric Sciences, Florida State University, Tallahassee FL 32306 USA.*
Claire Carvallo, *Institut de Minéralogie, de Physique des Matériaux et de Cosmochimie, Université Pierre et Marie Curie, 4 Place Jussieu, F-75005 Paris, France.*
Timothy Chapman, *School of Geosciences, University of Sydney, NSW 2006, Australia.*
Gail L. Christeson, *University of Texas Institute for Geophysics, Austin TX 78758-4445 USA.*
Eric C. Ferré, *Department of Geology Southern Illinois University, Carbondale IL 62901-4234 USA.*
Marguerite Godard, *Geosciences Montpellier- UMR 5243, Université Montpellier II, 34095 Montpellier, France.*
Daniel E. Heaton, *College of Earth, Ocean and Atmospheric Sciences, Oregon State University, Corvalis OR 97331-5503 USA.*
Maria Kirchenbaur, *Universität Kõln, Geologisches Institut, 50674 Koln, Germany.*
Walter Kurz, *Institute of Earth Sciences, University of Graz, A-8010 Graz, Austria.*
Steffen Kutterolf, *GEOMAR Helmholtz Centre for Ocean Research, 24148 Kiel Germany.*
Hongyan Li, *State Key Laboratory of Isotope Geochemistry, Guangzhou Institute of Geochemistry, Chinese Academy of Sciences, Guangzhou 510640, P.R. China.*
Yibing Li, *Institute of Geology, Chinese Academy of Geological Science, Beijing 100037, P.R. China.*
Katsuyoshi Michibayashi, *Institute of Geosciences, Shizuoka University, Shizuoka 422-8529 Japan.*
Sally Morgan, *Department of Geology, University of Leicester, Leicester LE1 7RH, United Kingdom.*
Wendy R. Nelson, *Department of Physics, Astronomy, and Geosciences, Towson University, Towson, MD 21252, USA.*
Julie Prytulak, *Department of Earth Science & Engineering, Imperial College London, London SW7 2AZ United Kingdom.*
Marie Python, *Department of Earth and Planetary Sciences, Hokkaido University, Hokkaido Sapporo 060-0810 Japan.*

Alastair H.F. Robertson, *School of Geosciences, University of Edinburgh, Edinburgh EH9 3JW United Kingdom.*
Jeffrey G. Ryan, *Department of Geology, University of South Florida, Tampa FL 33620 USA.*
William W. Sager, *Earth & Atmospheric Sciences, University of Houston, 127B Science and Research Building 1, Houston TX 77204 USA.*
Tetsuya Sakuyama, *Department of Science, Osaka University, Sumiyoshi-ku Osaka 558-8585 Japan*.
John W. Shervais, *Department of Geology, Utah State University, Logan UT 84322-4505 USA.*
Kenji Shimizu, *IFREE, JAMSTEC, 2-15 Natsushima-cho, Yokosuka 237-0061, Japan.*
Scott A. Whattam, *Department of Earth and Environmental Sciences, Korea University, Seoul 136-701, Republic of Korea.*

*Corresponding author.

Subduction Initiation and Ophiolite Crust: New Insights From IODP Drilling

Abstract

International Ocean Discovery Program (IODP) Expedition 352 recovered a high-fidelity record of volcanism related to subduction initiation in the Bonin fore-arc. Two sites (U1440 and U1441) located in deep water nearer to the trench recovered basalts and related rocks; two sites (U1439 and U1442) located in shallower water further from the trench recovered boninites and related rocks. Drilling in both areas ended in dolerites inferred to be sheeted intrusive rocks. The basalts apparently erupted immediately after subduction initiation and have compositions similar to those of the most depleted basalts generated by rapid sea-floor spreading at mid-ocean ridges, with little or no slab input. Subsequent melting to generate boninites involved more depleted mantle and hotter and deeper subducted components as subduction progressed and volcanism migrated away from the trench. This volcanic sequence is akin to that recorded by many ophiolites, supporting a direct link between subduction initiation, fore-arc spreading and ophiolite genesis.

Keywords: Izu, Bonin, boninite, basalt, drilling, IODP, Expedition 352, ophiolite, subduction initiation, Philippine plate

Introduction

The origin of ophiolites (oceanic lithosphere now exposed on land) has long been controversial. Though originally attributed to mid-ocean ridge settings (Thayer, 1969), the discovery of subduction-influenced lavas in some ophiolites suggested an island arc origin, inciting a long-running debate (e.g. Miyashiro, 1973; Gass, 1975; MacLeod et al., 2013). Continued study made it clear that subduction-affected lavas are widespread in ophiolites (e.g. Shervais, 1982), which led to the concept of supra-subduction zone (SSZ) ophiolites, defined as those formed at ridges above subduction zones rather than at mid-ocean ridges (Pearce et al., 1984). Current debate centers on the dynamics of SSZ ophiolite emplacement. One favored hypothesis relies on extension and hence generation of oceanic crust near an embryonic trench as a newly subducting plate rolls back (Stern and Bloomer, 1982; Nikolaeva et al., 2008; Whattam and Stern, 2011). In this scenario, SSZ ophiolites are generated immediately following subduction initiation and are preserved in fore-arcs (e.g. Dilek and Flower, 2003). However, for many SSZ ophiolites, sea-floor spreading in a back-arc setting has been considered a viable alternative scenario (e.g.

Meffre et al., 1996).

In support of a fore-arc setting for SSZ ophiolite genesis was the discovery, by diving and dredging, of abundant basalts (Johnson and Fryer, 1990; DeBari et al., 1999; Reagan et al., 2010; Ishizuka et al., 2011) and other lithologies commonly found in ophiolites (e.g. Bloomer, 1983) on the Izu-Bonin-Mariana (IBM) trench slope. These "fore-arc basalts" (FAB), as first defined in the Mariana fore-arc (Reagan et al., 2010) share many chemical and petrographic similarities with mid-ocean ridge basalts (MORB) and IBM back-arc basin lavas. However, most were derived from more depleted mantle sources, and some have compositions subtly influenced by subduction. FAB from the Bonin and Mariana fore-arcs yield ages around 51.5 Ma, which is thought to approximate the age of subduction initiation (Ishizuka et al., 2011; Reagan et al., 2013).

Boninite samples were collected mostly upslope from FAB (e.g. Ishizuka et al., 2011), and crop out subaerially at their type locality on Chichijima in the Bonin Islands (Umino, 1985). Boninites are relatively rare high-Mg andesites with exceedingly low concentrations of Ti and rare-earth elements, and relatively high concentrations of fluid mobile elements (Taylor et al., 1994) and water (Dobson, 1987). They are found in some subduction zones and ophiolites where extensive melting of the mantle occurred at shallow depths because of strong water fluxing (e.g. Crawford et al., 1989). In the IBM fore-arc, boninites are younger than FAB, with ages of 49 to 43 Ma (Ishizuka et al., 2006). DSDP Site 458 in the Mariana fore-arc drilled lavas with compositions that are transitional between FAB and boninite (Reagan et al., 2010). One boninitic lava was dated at 49.3 Ma (Cosca et al., 1998).

IODP Expedition 352 (Reagan et al., 2015a) was targeted to drill a complete volcanic reference section in the Bonin fore-arc to test models of ophiolite genesis and to explore early subduction dynamics. Drill sites were located (Fig. 1) where fragmentary results of submersible diving alluded to a broadly ophiolitic stratigraphy including FAB and boninite (Ishizuka et al., 2011). The drilling plan called for two sites. Site U1439 was drilled at ~3100 m water depth, and aimed to core from boninite downward to FAB lavas. Site U1440 was located ~15 km closer to the trench at ~4800 m water depth, and aimed to sample from FAB lavas to sheeted dikes. By drilling in the casing in Holes U1439C and U1440B (see Reagan et al., 2015), enough time was saved to allow coring at two additional sites, U1441 and U1442, which recovered additional

sections of FAB and boninite lavas respectively. When considered together with DSDP Site 458, the drilling results provide the first complete representation of the volcanic stratigraphy at an in-situ and intact fore-arc generated during subduction initiation.

Methods

The methods employed onboard the JOIDES Resolution during IODP Expedition 352 for core analysis are discussed in detail in Reagan et al. (2015) and Ryan et al. (2016). Techniques for onboard whole rock analyses are summarized here. Rock samples were cut from cores using a diamond-blade rock saw. Outer surfaces of rock samples were removed before samples were cleaned with isopropanol and deionized water (18 MΩ) and dried for 10 min. Rocks were crushed then ground to a fine powder using a tungsten carbide mill. An aliquot of the sample powder was ignited for 4 h at 1025°C to determine weight loss on ignition (LOI), with an estimated precision of 0.02 g (0.4%). Splits of ignited whole-rock powders were mixed with $LiBO_2$ flux and fused in Pt-Au crucibles. The resulting beads were dissolved in 50 mL of a 10% HNO_3 solution. The solutions were filtered and diluted to a 2000:1 dilution with a 10% HNO_3 solution that included 10 ppm Ge and 1000 ppm Li. These solutions were analyzed for major elements and key trace elements using a Teledyne Leeman Labs Prodigy ICP-AES instrument. Reference materials used in data calibration included: JP-1, BIR-1, BCR-2, MRG-1, AGV-1, and JG-1A. Basalt standard BHVO-2 was used to monitor instrument drift and as well as a secondary standard for calibration. Basalt BHVO-2 and three previously analyzed boninite samples from Chichijima Island (Samples X88, 40618, and 32108; J. Pearce, pers. comm., 2014) were run frequently as unknowns to track reproducibility. A discussion of detection limits, accuracy and reproducibility of the chemical species analyzed via shipboard ICP-AES methods may be found in Reagan et al. (2015).

Cut core surfaces were analyzed quantitatively for key elements using a Thermo Fisher Niton XL3t GOLDD+ portable energy-dispersive XRF instrument. The ability to accurate analyze essentially unprocessed samples for several important elements allowed essentially real time assessment of rock compositions during coring. Samples were mounted in a uniform geometry with respect to the instrument using a Niton Field-Mate sample holder system, or an IODP-constructed system designed to handle long core segments. The “Soils” analytical protocol was used for all analyses. Individual pXRF measurements were 60 seconds in duration, with an

average of three measurements from closely adjacent spots on as sample surface constituting a single analysis. The BHVO-2 basaltic reference material was analyzed with each set of unknowns to track instrument performance, and repeated measurements indicated no significant instrument signal drift and ±3% overall uncertainty for higher precision elements over the course of the expedition. Calibration curves were constructed based on powder mounts of the standards BHVO-2; BCR-2, JB-2, JB-3, AGV-1, MRG-1, JP-1, and DTS-1, along with the three analyzed Chichijima boninites, which helped extend the ranges of working curves for Cr and other key elements. Instrument performance was tested and found to be indistinguishable for analyses of powder mounts and of rock surfaces, and tests at multiple positions on rock surfaces were found to be similar within instrument uncertainties for Expedition 352 basalts and boninites, and for Mariana fore-arc volcanic samples previously analyzed by Reagan et al (2010). Elements found to have good accuracy and reproducibility using these methods were: TiO_2, CaO, K_2O, Rb, Sr, Zn, Cu, Cr, V, and Zr (see Ryan et al., 2016 for a detailed discussion of detection limits, accuracy and reproducibility).

FAB Sites U1440 and U1441

The main penetration through basement was at Hole U1440B. Here, ~5 m of talus is underlain by over 175 m of basaltic pillow lavas, sheet flows, and hyaloclastites (Fig. 2). These are in turn underlain by 70 m of lavas interspersed with dolerite dikes or sills, before ending in 40 m of entirely shallow intrusive rocks representing multiple intrusions. By reference to equivalent sequences in oceanic crust and ophiolites (e.g. Langmuir et al., 1986; Detrick et al., 1994; Hekinian et al., 1995), we treat this as an indicator that the hole bottomed in dikes and that the entire extant FAB lava sequence at this location was likely drilled. The second site drilled at in Hole U1441A had significantly less penetration, encountering about 55 m of variably depleted FAB beneath about 70 m of talus with FAB clasts.

The chemical compositions of the igneous rocks cored at Sites U1440 and U1441 are similar to one another and to FAB from dives in the IBM fore-arc (Reagan et al., 2010; Ishizuka et al., 2011). Almost all of the lavas and dikes classify as tholeiitic basalts by standard IUGS criteria (Le Bas, 2000). Exceptions at Site U1440 are rare basaltic andesites, and one thin glass-rich andesite (Fig. 3). These andesitic lavas have major and trace element compositions consistent with genesis by differentiation of FAB. FABs from the drill core and elsewhere in the IBM fore-

arc have MORB-like MgO concentrations (5 - 9 wt%.). Petrographically, the basalts from Sites U1440 and U1441 are aphyric to sparsely plagioclase or augite phyric with glassy to microcrystalline plagioclase-augite–magnetite groundmasses (Fig. 4A,B) and low vesicularity (0 to 5%). Dolerites have chemical compositions like FAB and were recognized by their subophitic textures.

Concentrations of the petrogenetically useful elements listed above that were collected onboard using the shipboard portable XRF instrument (Ryan et al., 2016) were key to understanding how source compositions, melting processes, and degrees of differentiation changed through time. Although FABs are similar to MORB in their major element composition, they have higher average Ti/Zr (Fig. 5), reflecting their depleted sources (Reagan et al., 2010). In terms of ratios of more (Sr) to less (Zr) subduction-mobile elements, most FAB and some basal dolerites have Sr/Zr ratios within the range of MORB glasses (Fig. 5). Some samples do, however, have Sr/Zr values clearly above those of MORB glasses, even the most highly depleted MORB glasses, such as those from the Carlsberg Ridge (cf. Jenner and O'Neill, 2012). The relatively high Sr concentrations in these samples are consistent with a subduction-influence, although an enrichment in Sr during post-emplacement alteration cannot be definitively ruled out by the whole-rock concentration data alone. Samples from about 170 m below seafloor in Hole U1441A, herein termed depleted or D-FAB, have particularly high Sr/Zr and Ti/Zr (c. 3.2 and 220 respectively, Fig. 5), low incompatible trace element abundances, and high CaO concentrations (see Supplementary Materials Table S2), likely reflecting water-enhanced melting of a strongly depleted source.

Chromium concentrations are moderate to low and generally decrease upwards in the lavas from both FAB holes, reflecting increased fractionation of Cr-bearing phases up-section (Fig. 2). These overall trends are disrupted by narrow sections of core with significantly more, or less, fractionated lavas. The D-FABs from Hole U1441A have the highest Cr concentrations and are the least fractionated of any lava at both sites.

Boninite Sites U1439 and U1442

The igneous basement at both sites consists of pillow lavas, massive sheet flows, hyaloclastites, subaqueous pyroclastic flow deposits, and other igneous breccias. Both sites, particularly Site U1442, have more hyaloclastites than do the FAB sites (Fig. 6). In several cores at both sites,

more and less differentiated magmas appear to have erupted simultaneously, forming complex magma mingling textures in pillow lavas. The lowermost unit of Site U1439 is ~50 m of fine-grained dolerite that is interpreted to be intrusive, and could represent a dike complex. In contrast to Hole U1440B, the boninite dikes have some chilled margins and rare lava screens. No FAB was found beneath boninite in these screens.

The boninite lavas drilled at Sites U1439 and U1442 are chemically distinct from FAB. Virtually all samples from Sites U1439 and U1442 plot in the boninite field defined by the IUGS (see Fig. 3) or its extrapolation to more evolved compositions (Pearce and Robinson, 2010). The boninite field was subdivided based on our shipboard results into low-Si and high-Si boninite following the concept of Kanayama et al. (2013). The high-Si boninites are akin to the low-Ca boninites (Crawford et al., 1989) from Chichijima, whereas low-Si boninites have compositions similar to those of boninitic lavas from DSDP Site 458 (e.g. Meijer et al., 1981). Some samples were given a shipboard classification of "basaltic boninites" because they had boninitic trace element compositions (i.e. low Ti/Zr and TiO_2 concentrations, high Sr/Zr) but basaltic SiO_2 concentrations. Differentiated high-Mg andesites that follow liquid lines of descent from parental boninites were considered to be boninite-series lavas.

Boninites also are petrographically distinct from FAB, as they are typically highly vesicular and porphyritic. Low-Si and basaltic series boninites (Fig 4C,D) have phenocrysts of olivine, pyroxenes, and rare plagioclase and chromite in a matrix with abundant microlites of clinopyroxene +/- plagioclase. High-Si boninites (Fig. 4E,F) typically have abundant phenocrysts of orthopyroxene and/or olivine in a glassy matrix with pyroxene microlites.

Sites U1439 and U1442 have chemostratigraphic similarities, but also differences that are surprisingly great considering they are only ~1.3 km apart. Lavas from both sites have more primitive compositions upward based on Cr concentrations. Highly evolved low-Si to basaltic boninite-series lavas with low Cr concentrations make up more than half of the material recovered at Site U1442 but only 20 m at the base of the lava sequence at Site U1439 (Fig. 6). Overlying the basal differentiated lavas at both sites are units dominated by low-Si boninite series lavas with highly variable Cr concentrations, indicating that some magmas underwent significant crystal fractionation, whereas others rose to the surface essentially unfractionated. Mingling between magmas with high- and low-Cr concentrations is common in this unit. A

compositional excursion to relatively unfractionated basaltic boninite-series lavas is present from 251 to 282 mbsf in Site U1439. High-Si boninites cap both sites. Most of these lavas are relatively primitive, with Cr concentrations of 200–1600 ppm and MgO of 9–17 wt% (see Supplementary Materials Table S2).

The extreme depletion of the mantle sources and degrees of melting for all boninite lavas is reflected in their low TiO_2 concentrations (Fig. 3). This is particularly true of high-Si boninites, which have TiO_2 <0.26 wt%. However, although Ti/Zr typically increases in magmas with increasing mantle melting, Ti/Zr ratios are lowest in these high-Si boninites (Fig. 5), possibly reflecting mobilization of Zr in a slab-melt subduction component (Pearce et al., 1992). Sr/Zr ratios are nonetheless high in all boninites, providing clear evidence for a significant involvement of a mass flux from a subducting plate during magma genesis.

Discussion and Conclusions

FAB Sites U1440 and U1441 drilled basaltic oceanic crust that likely formed at a ridge with a robust melt supply and an underlying dike swarm. This view is supported by: [A] multiple sheeted intrusions below oceanic lavas and hyaloclastites (cf. Detrick et al., 1994), [B] the evolved nature of the intrusions and lavas (cf. Langmuir et al., 1986, Sano et al., 2011), [C] the increased fractionation up-section of the latter (cf. Expedition 309/312 Scientists, 2006), [D] the presence trenchward of the full ophiolite spectrum from lavas to peridotites (Ishizuka et al., 2011), and [E] geodynamic modeling indicating that subduction initiation can result in rapid roll-back of the slab and the generation of large tracts of oceanic lithosphere (e.g. Hall et al., 2003; Leng et al., 2012). Evidence that this lithosphere formed specifically in a subduction initiation setting, rather than having been accreted from the Pacific Plate or representing pre-subduction spreading on the Philippine Sea Plate, includes: [A] the chemical and spatial association of FAB lavas and dikes with a 2400 km long trench-parallel province of volcanic and plutonic rocks dated at ~51.5 Ma (Ishizuka et al., 2011; Reagan et al., 2013), [B] the potential involvement of subducted fluids in the genesis of some intercalated lavas from Sites U1440 and U1441 (e.g. D-FAB), [C] the low Ti/V ratios for FAB from the IBM, likely reflecting a higher oxygen fugacity (Shervais, 1982) or enhanced melting (Reagan et al., 2010) than is normally prevalent at mid-ocean ridges, and [D] the continuity of magma compositions between the FAB sites, DSDP Site

458, the boninite sites (Fig. 3) and on-land exposures of the Ogasawara Ridge suggesting a genetic link.

The apparent dike swarm under FAB suggests moderate to fast spreading rates (e.g. Sinton and Detrick, 1992; Marjanović et al., 2014), but some caution is needed (Robinson et al., 2008). At mid-ocean ridges, the magma supply is related to rates of spreading and extension-driven decompression, with mantle potential temperature being the principal independent variable (e.g. McKenzie and Bickle, 1988). For subduction initiation ridges, mantle temperature can be more complex because of the potential for rapid influx of mantle and the presence of a cold subducting plate. Subducted water is additionally able to increase magma supply (and hence likelihood of a dike swarm) for a given spreading rate (e.g. Kelley et al., 2006; Langmuir et al., 2006), and enhanced mantle depletion can potentially reduce magma supply. The differentiated nature of FAB and likely presence of an underlying dike swarm suggest that conditions balanced to generate enough magma to maintain a fractionating crystal mush – melt lens complex and basaltic crust production (cf. Marjanović, et al., 2014) during sea-floor spreading related to subduction initiation in the IBM.

As in the FAB section, the uniformly low Cr and MgO concentrations in the lowermost lavas in the boninite holes suggest persistently fractionating magmas and continued sea-floor spreading. However, in contrast with the FAB section, relatively primitive lavas are common up-section, illustrating that persistent fractionation of melt at a ridge axis gave way to ephemeral fractionating magma bodies.

Melting to generate boninites probably occurred at lower potential temperatures than for FAB (Langmuir et al., 2006; Lee et al., 2009), which would be expected if boninite sources are residues from the genesis of FAB. Moreover, the low Ti and REE contents of the boninite lavas indicate that their sources are strongly depleted (Pearce et al., 1992). Melt productivity, therefore, depends on the balance between the extra melting associated with water fluxing and reduced productivity because of mantle depletion and potential temperature. Adding 1 wt% of subducted water to the mantle sources for the modern Mariana arc produces about 20% melting above that generated by decompression (Kelley et al., 2006), and it is likely that a similar enhancement of productivity while generating boninites made up for melt volume lost by

depletion and a fall in temperature. In this case, the presence of a dike swarm manifests a balance not between rate of extension and rate of melt generation as at ocean ridges, but between the much less quantifiable rate of fluid release from the slab and rate of continued slab rollback. Once the latter decreases, the likely result will be a transition from spreading to focused protoarc volcanism. The boninite sites have a stratigraphic record that might reflect this transition.

There are two ways in which FAB genesis could have transitioned to boninite genesis over time and away from the trench. First, the spreading center creating FAB crust might have extended well to the west beyond Site U1439, followed by a ridge jump back towards the trench to create boninitic crust. Alternatively, the original spreading center could have transitioned directly from generating FAB crust to generating boninite crust. The second of these explanations is favored by the presence of the full transition from FAB to boninite represented in the drill cores from Expedition 352 combined with those from DSDP Site 458 (Fig. 5).

Fig. 7 illustrates how we envisage the evolution of the ocean basin from inception of subduction at a transform margin (Fig. 7a) through to the end of spreading and the start of development of the earliest arc, or 'protoarc' (Fig. 7d). When subduction begins (Fig. 7b), extension related to rollback produces FAB crust. At this point, magmas are generated from a depleted mantle source that has advected into the wedge in response to rollback-driven suction and which melts in response to decompression. The depleted nature of FAB sources reflects an inherent original depletion above that of normal MORB sources (e.g. Reagan et al., 2010). The most depleted FAB (e.g. D-FAB) compositions are the result of additional melting of this source caused by fluid addition from the subducting plate. The limited involvement of subducted fluids in FAB genesis reflects the insufficient time to effectively transfer heat and mass between the newly subducting plate and the overlying mantle. The succession from largely decompression melting to largely flux melting farther from the trench (Fig. 7c) can be explained by the progressive increase with time in the depth of the newly subducting plate and the temperature at the slab-wedge interface, both of which will significantly increase the flux of subducted water and other constituents. The mantle source depletion must have increased together with this flux effect to produce boninites rather than basalts. Boninite generation likely starts near the slab-wedge interface. One model has water-rich melts that are generated at the interface migrating upward in high porosity channels, promoting continued flux-melting of residual FAB-source

mantle in the channel (e.g. Grove et al., 2003). Alternatively, boninites might be generated from relatively cool mantle diapirs from a depleted thermal slab-wedge boundary layer enriched in subducted constituents (Nikolaeva et al., 2008), which melts by rising through the hotter mantle wedge. In either case, a key point made by Fig. 7 is that depleted, and hence buoyant, residue from FAB melting did not escape from the mantle wedge before wedge-slab coupling was established by deep subduction.

The final event recorded by the drilling was the change to more primitive boninites up-section at Sites U1439 and U1442. In keeping with the model illustrated in Fig. 7d, one plausible hypothesis is that spreading rates declined, which inhibited development of an axial mush-melt lens system (e.g. Dick, 1989). Thus, the upper boninite group lavas may be viewed as representing the transition between early sea-floor spreading and the start of the protoarc with its focused magmatism. A particular point of significance for ophiolite comparisons is that the subduction input increased *away* from the trench, not towards it as in rear-arc settings (e.g. Hochstaedter et al., 2001). Another is the presence of high-Si boninites above low-Si and basaltic boninites at the drill sites. High-Si boninites are particularly rare lavas and, for modern-day, in-situ oceanic crust, they have only so far been found in preserved fore-arcs related to subduction initiation. Their presence in ophiolitic terranes, especially at the end of an overall time progression from FAB to high-Si boninite, could represent a direct link to a subduction initiation environment.

Site U1438 drilled during IODP Expedition 351 intersected basalts beneath Eocene sediments (Arculus et al., 2015). These basalts resemble FAB from Sites U1440 and U1441, but are less depleted in incompatible trace element concentrations. Although the ages of these lavas remain uncertain, Arculus et al (2015) hypothesized that they are FAB equivalents in the far back-arc. If so, then these basalts could represent the west side of the spreading center illustrated in Fig. 7, where their greater fertility would be in keeping with their genesis before the basalts drilled at Sites U1440 and U1441 when the nascent mantle wedge was less depleted. Sediment ages at Site U1438 (Arculus et al., 2015) allow its basement basalts to be younger than FAB. Thus, an alternative setting for their eruption could have been in an early back-arc basin that developed while boninitic volcanism was focusing in the area near Sites U1439 and U1442 and the Bonin fore-arc islands. Regardless of whether the basement at Site U1438 is equivalent to

FAB, the western microplate created during spreading was largely integrated into the crust beneath the Kyushu-Palau ridge and Izu-Bonin arc. The less depleted basaltic crust that could have been the mirror image of the western microplate would have been east of Site U1440 where peridotites now crop out on the ocean floor (Ishizuka et al., 2011). We hypothesize that this nascent crust was later removed, for example, by trenchward gravity collapse and subduction.

Acknowledgments

This research used samples and data provided by the International Ocean Discovery Program. We thank all the personnel aboard the JOIDES Resolution during Expedition 352 for their skill and dedication. Particular thanks go to the Technical Support staff for the quality and timeliness of their work. Stephen Midgley deserves special recognition for his recommendation to drill in casing, which allowed the final two holes to be drilled. We gratefully acknowledge Bob Stern, Osamu Ishizuka, and the other drilling proposal proponents for making Expedition 352 possible. We thank the USSSP for initial funding of US scientists, and NSF grants OCE1558608 (Nelson), OCE1558647 (Reagan), OCE1558689 (Shervais), and OCR1558855 (Ryan), for continued funding. J. Prytulak was supported by NERC grant NE/M010643. S. Kutterolf thanks the German Research Foundation (KU-2685/4-1), and R. Almeev thanks the German Science Foundation (DFG Project AL 1189/8) for financial support. W. Kurz was supported by the Austrian Academy of Sciences and by the Austrian Science Fund (FWF Project P27982-N29). K. Michibayashi was supported by the Japan Society for the Promotion of Science and the Japan Drilling Earth Science Consortium. H.Y. Li acknowledges the support from the State Oceanic Administration (GASI-GEOGE-02). T. Chapman was funded by ANZIC. A constructive review by Matthew Loocke and editorial comments by Bob Stern significantly improved the manuscript.

References

Arculus, R.J., Ishizuka, O., Bogus, K.A., Gurnis, M., Hickey-Vargas, R., et. al., 2015, A record of spontaneous subduction initiation in the Izu-Bonin-Mariana arc. Nature Geoscience, v. 8, p. 728–733. doi:10.1038/ngeo2515.

Bloomer, S.H. 1983, Distribution and origin of igneous rocks from the landward slopes of the Mariana Trench; implications for its structure and evolution: Journal of Geophysical Research, v. 88, p. 7411-7428.

Crawford, A.J., Falloon, T.J., and Green, D.H., 1989, Classification, petrogenesis and tectonic setting of boninites. In Boninites, London, United Kingdom (GBR): Unwin Hyman, p. 1-49.

Cosca, M.A., Arculus, R.J., Pearce, J.A., and Mitchell, J.G., 1998, 40Ar/39Ar and K-Ar geochronological age constraints for the inception and early evolution of the Izu-Bonin-Mariana arc system. Island Arc, v. 7, p. 579–595.

DeBari, S.M., Taylor, B., Spencer, K., and Fujioka, K., 1999. A trapped Philippine Sea Plate origin for MORB from the inner slope of the Izu-Bonin Trench. Earth and Planetary Science Letters, v. 174, p. 183-197.

Detrick, R., Collins, J., Stephen, R., and Swift, S., 1994, In situ evidence for the nature of the seismic layer 2/3 boundary in oceanic crust: Nature (London), v. 370, p. 288-290.

Dick, H. J. B., 1989, Abyssal peridotites, very slow spreading ridges and ocean ridge magmatism. Geological Society of London, Special Publications, v. 42, p. 71-105.

Dilek, Y., Flower, M.F.J., 2003, Arc-trench rollback and forearc accretion; 2, A model template for ophiolites in Albania, Cyprus, and Oman. Geological Society Special Publications, v. 218 p. 43-68.

Dobson, P.F., and O'Neil, J.R., 1987, *Stable isotope compositions and water contents of boninite series volcanic rocks from Chichi-jima, Bonin Islands, Japan:* Earth and Planetary Science Letters*, v. 82, p. 75-86.*

Expedition 309/312 Scientists, 2006, Expedition 309/312 summary. In Teagle, D.A.H., Alt, J.C., Umino, S., Miyashita, S., Banerjee, N.R., Wilson, D.S., and the Expedition 309/312 Scientists. Proceedings IODP, v. 309/312: Washington, DC (Integrated Ocean Drilling Program Management International, Inc.), p. 1–127. doi:10.2204/iodp.proc.309312.101.2006.

Gass, I.G., Neary, C R, Plant, J., Robertson, A.H.F., and Simonian, K.O., 1975, Comments on "The Troodos ophiolitic complex was probably formed in an island arc", by A. Miyashiro and subsequent correspondence by A. Hynes and A. Miyashiro: Earth and Planetary Science Letters v. 25, p. 236-238.

Grove, T.L., Elkins-Tanton, L.T., Parman S.W., Chatterjee, N., Müntener, O., and Gaetani, G.A., 2003, Fractional crystallization and mantle-melting controls on calc-alkaline differentiation trends: Contributions to Mineralogy and Petrology, v. 145, p. 515–533. doi:10.1007/s00410-003-0448-z.

Hall, C.E., Gurnis, M., Sdrolias, M., Lavier, L.L., and Mueller, R.D., 2003, Catastrophic initiation of subduction following forced convergence across fracture zones: Earth and Planetary Science Letters, v. 212, p. 15-30.

Hekinian, R., Bideau, D., Hebert, R., and Niu, Y., 2006, Magmatism in the Garrett transform fault (East Pacific Rise near 13 degrees 27'S): Journal of Geophysical Researchv. v. 100B, p. 10,163-10,185.

Hochstaedter, A., Gill, J., Peters, R., Broughton, P., Holden, P., and Taylor, B., 2001, Across-arc geochemical trends in the Izu-Bonin arc: Contributions from the subducting slab. Geochemistry, Geophysics, Geosystems, v. 2, p. 1-44, doi: 10.1029/2000GC000105.

Ishizuka, O., Kimura ,J-I., Li, Y.B., Stern, R.J., Reagan, M.K., Taylor, R.N., Ohara, Y., Bloomer, S.H., Ishii, T., Hargrove III, U.S., and Haraguchi, S., 2006, Early stages in the evolution of Izu–Bonin arc volcanism: New age, chemical, and isotopic constraints: Earth and Planetary Science Letters, v. 250, p. 385-401.

Ishizuka, O., Tani, K., Reagan, M.K., Kanayama, K., Umino, S., Harigane, Y., Sakamoto, I., Miyajima, Y., Yuasa, M., Dunkley, D.J., 2011, The timescales of subduction initiation and subsequent evolution of an oceanic island arc: Earth and Planetary Science Letters, v. 306 p. 229-240.

Jenner, F.E., and O'Neill, H.St.C., 2012, Analysis of 60 elements in 616 ocean floor basaltic glasses: Geochemistry, Geophysics, Geosystems, v. 13, p. 1-11, doi:10.1029/2011GC004009.

Johnson, L.E., and Fryer, P., 1990, The first evidence for MORB-like lavas from the outer Mariana forearc; geochemistry, petrography and tectonic implications: Earth and Planetary Science Letters, v. 100, p. 304-316.

Kanayama, K., Katmura, K., and Umino, S., 2013, New geochemical classification of global boninites: IAVCEI 2013 Scientific Assembly Abstract 4W-1B-P13.

Kelley, K.A., Plank, T., Newman, S., Stolper, E., Grove, T.L., and Hauri, E., 2006. Mantle melting as a function of water content at subduction zones. I: back-arc basins: Journal of Geophysical Research, v. 111, p. 1-27, doi: 10.1029/2005JB003732.

Langmuir, C.H., Bender, J.F., and Batiza, R., 1986, Petrological and tectonic segmentation of the East Pacific Rise, 5 degrees 30'-14 degrees 30'N: Nature (London), v. 322, p. 422-429.

Langmuir, C.H., Bézos A., Escrig S., and Parman S.W., 2006, Chemical systematics and hydrous melting of the mantle in back-arc basins. In: Christie D.M., Fisher C.R., editors. Back-arc Spreading Systems: Geological, Biological, Chemical, and Physical Interactions. Geophysical Monograph, American Geophysical Union. v. 166. p. 87-146.

Le Bas, M J., 2000, IUGS reclassification of the high-Mg and picritic volcanic rocks: Journal of Petrology, v. 41, p. 1467-1470.

Lee, C-T.A., Luffi, P., Plank, T., Dalton, H., and Leeman, W.P., 2009, Constraints on the depths and temperatures of basaltic magma generation on Earth and other terrestrial planets using new thermobarometers: Earth and Planetary Science Letters, v. 279, p. 20-33. doi:10.1016/j.epsl.2008.12.020.

Leng, W., Gurnis, M. and Asimow, P., 2012, From basalts to boninites; the geodynamics of volcanic expression during induced subduction initiation: Lithosphere, v. 4, p. 511-523.

MacLeod, C.J., Lissenberg, C.J. and Bibby, L.E., 2013, 'Moist MORB' axial magmatism in the Oman ophiolite: The evidence against a mid-ocean ridge origin. Geology, v, 41, p, 459–462.

Marjanović, M., Carbotte, S.M., Carton, H., Nedimović, M.R., Mutter, J.C., and Canales, J.P., 2014, A multi-sill magma plumbing system beneath the axis of the East Pacific Rise. Nature Geoscience, v. 7, p. 825-829.

McKenzie, D., and Bickle, M J., 1988, The volume and composition of melt generated by extension of the lithosphere: Journal of Petrology, v. 29., p. 625-679.

Meffre, S., Aitchison, J.C., and Crawford, A.J., Geochemical evolution and tectonic significance of boninites and tholeiites from the Koh Ophiolite, New Caledonia: Tectonics, v. 15, p. 67-83.

Meijer, A., Anthony, E., and Reagan, M., 1982, Petrology of volcanic rocks from the fore-arc sites: Initial Reports of DSDP, v. 60, p. 709–729.

Miyashiro, A., 1973, The Troodos ophiolitic complex was probably formed in an island arc: Earth and Planetary Science Letters, v. 19, p. 218-224.

Nikolaeva, K., Gerya, T.V., and Connolly, J.A.D., 2008, Numerical modelling of crustal growth in intraoceanic volcanic arcs: Physics of the Earth and Planetary Interiors, v. 171, p. 336-356.

Parman, S.W., and Grove, T.L, 2004, Harzburgite melting with and without H_2O: experimental data and predictive modeling: Journal of Geophysical Research. v. 109B, p. 1-20,.doi:10.1029/2003JB002566.

Pearce J.A., van der Laan, S.R., Arculus, R.J., Murton, B.J., Ishii, T., Peate, D.W., and Parkinson, I.J., 1992, Boninite and harzburgite from Leg 125 (Bonin-Mariana forearc): A case study of magma genesis during the initial stages of subduction: Proceedings ODP, Scientific Results, v. 125 p. 623–659.

Pearce, J.A., and Robinson, P.T., 2010, The Troodos ophiolitic complex probably formed in a subduction initiation, slab edge setting: Gondwana Research, v. 18, p. 60-81.

Pearce, J.A., Lippard, S.J., and Roberts, S., 1984, Characteristics and tectonic significance of supra-subduction zone ophiolites: Geological Society Special Publications, v.16, p. 74-94.

Reagan, M.K., Ishizuka, O., Stern, R.J., Kelley, K.A., Ohara, Y., Blichert-Toft, J., Bloomer, S.H., Cash, J., Fryer, P., Hanan, B., Hickey-Vargas, R., Ishii, T., Kimura, J-I., Peate, D.W., Rowe, M.C., and Woods, M., 2010, Fore-arc basalts and subduction initiation in the Izu-Bonin-Mariana system: Geochemistry Geophysics Geosystems. v. 11, p. 1-17, doi: 10.1029/2009GC002871.

Reagan, M.K., McClelland, W.C. Girard, G., Goff, K.R., Peate, D.W., Ohara, Y., and Stern, R.J., 2013, The geology of the southern Mariana fore-arc crust: implications for the scale of Eocene volcanism in the western Pacific. Earth and Planetary Science Letters, v. 380, p. 41-51.

Reagan, M.K., Pearce, J.A., Petronotis, K., and Expedition Scientists, 2015, Izu-Bonin-Mariana Fore Arc. Proceedings of the International Ocean Discovery Program, 352. International Ocean Discovery Program. http://dx.doi.org/10.14379/iodp.proc.352.2015.

Robinson, P.T., Malpas, J., Dilek, Y., and Zhou, M-F., 2008, The significance of sheeted dike complexes in ophiolites: GSA Today, v. 18, p. 4-10.

Ryan, J.G., Li, Y., Reagan, M.K., Li, H., Heaton, D., Godard, M., Kirchenbaur, M., Whattam, S., Pearce, J.A., Chapman, T., Nelson, W., Prytulak, J., Shervais, J., Shimizu, K., Petronotis, K., and the IODP Expedition 352 Scientific Team, 2016 Application of a handheld X-ray fluorescence spectrometer for real-time, high-density quantitative analysis

of drilled igneous rocks and sediments during IODP Expedition 352: Chemical Geology (submitted).

Sano, T., Sakuyama, T., Ingle, S., Rodriguez, S., and Yamasaki, T., 2011, Petrological relationships among lavas, dikes, and gabbros from Integrated Ocean Drilling Program Hole 1256D: Insight into the magma plumbing system beneath the East Pacific Rise. Geochemistry Geophysics Geosystems. v. 12, p. 1-26, doi: 10.1029/2011GC003548.

Shervais, J.W., 1982, Ti-V plots and the petrogenesis of modern and ophiolitic lavas: Earth and Planetary Science Letters, v. 59, p. 101-118.

Sinton, J.M., and Detrick, R.S., Mid-ocean ridge magma chambers: Journal of Geophysical Research, v. 97p. 197-216.

Stern, R.J., and Bloomer, S.H., 1992, Subduction zone infancy; examples from the Eocene Izu-Bonin-Mariana and Jurassic California arcs: Geological Society of America Bulletin, v. 104, p. 1621-1636.

Taylor, R.N., Nesbitt, R.W., Vidal, P., Harmon, R., Auvray, B., et al., 1994, Mineralogy, chemistry, and genesis of the boninite series volcanics, Chichijima, Bonin Islands, Japan: Journal of Petrology, v. 35, p. 577-617.

Thayer, T.P., 1969, Peridotite-gabbro complexes as keys to petrology of mid-oceanic ridges: Geological Society of America Bulletin, v. 80, p. 1515-1522.

Umino, S., 1985, Volcanic geology of Chichijima, the Bonin Islands (Ogasawara Islands): Journal of the Geological Society of Japan, v. 91, p. 505-523.

Whattam, S.A., and Stern, R.J., 2011, The "subduction initiation rule"; a key for linking ophiolites, intra-oceanic fore-arcs, and subduction initiation: Contributions to Mineralogy and Petrology, v. 162, p. 1031-1045.

Figure Captions

Figure 1. Location map for Expedition 352 Sites U1439–U1442, and Shinkai 6500 dive sites in the Bonin fore-arc (Ishizuka et al., 2011) illustrating the encountered rock types. Also shown in the inset is the site for Expedition 351 Site U1438, which encountered basalts that have been postulated to be the equivalent to FAB (Arculus et al., 2015).

Figure 2. Representative stratigraphy and Cr concentrations with depth collected using the pXRF instrument (data from Supplementary Material Table S1) for samples from Holes U1440B and U1441A. “Transitional” indicates core with lavas and dikes/sills.

Figure 3. (A) MgO vs. SiO_2 and (B) TiO_2 vs. MgO diagrams were used to classify the volcanic rocks and dikes sampled during Expedition 352. Data were collected onboard by ICP-AES techniques (see Supplementary Material Table S2). Boninites (sensu stricto) are defined by IUGS (Le Bas, 2000) as having MgO > 8 wt%, TiO_2 < 0.5 wt%, and SiO_2 > 52 wt%, and so plot in the shaded rectangular fields on both diagrams. The dividing line between the boninite and the

basalt-andesite-dacite-rhyolite (BADR) series is from Pearce and Robinson (2010) (trans. = transitional). Differentiated low-Si boninite (L), high-Si boninite (H), and basaltic boninite (B). with MgO concentrations < 8 wt. % are classified as high-Mg andesites (HMA) in the fields shown. The color scheme used for the symbols is from the stratigraphic columns in Figs. 2 and 5.

Figure 4. Photomicrographs of thin sections from IODP Expedition 352. (A) and (B) are a cross-polar and plane polar images, respectively, of a pillow core clast from Core U1440A-13X-1-W 10/13. It is aphyric, consisting of a quench texture groundmass of plagioclase, clinopyroxene, magnetite, and altered glass. (C) and (D) are a cross polar and plane polar images, respectively of a glassy low-Si boninite found in Core U1439C-31R-3-W 66/69. It is a vesicular pillow rind with phenocrysts of olivine with chromite and glass inclusions. The groundmass consists of partially altered glass, chromite microphenocrysts, and quench clinopyroxene. Note the calcite filled vesicles at the base of the images. (E) and (F) are cross-polar and plane-polarized images, respectively, of a high-Si boninite hyaloclastite from Core U1439A-21X-CC-W 22/25. It consists of phenocrysts and quench crystals of orthopyroxene in a glassy matrix.

Figure 5. Plot of Sr/Zr vs. Ti/Zr collected by pXRF for cores from Expedition 352 and onboard cores from DSDP Site 458 (data from Supplementary Materials Table S1). All data were collected using the onboard pXRF. The andesite ("and") from Site U1440 and D-FAB compositions are highlighted. The yellow field represents MORB glass compositions. The red field labeled CR encompasses glass compositions from the Carlsberg Ridge (Jenner and O'Neill, 2012).

Figure 6. Representative stratigraphy and Cr concentrations collected by pXRF with depth for Holes U1439C and U1442A (data from Supplementary Material Table S1). To define boundaries of major lithostratigraphic units, we used correlations between Ti/Zr values collected by pXRF and the rock types illustrated in Fig. 3. High-Si, low-Si, and basaltic boninites were generally found to have Ti/Zr = 40-60, 60-95, and 90-120 respectively. With the exception of the high-Si boninites atop both holes, most units have minor interlayered strata with other boninitic compositions.

Figure 7. Creation and evolution of the Bonin crust after subduction initiation at about 52 Ma as inferred from Expedition 352. The initial plates are the Proto-Philippine Plate (PPP) and the Pacific plate (PAC). The developing IBM fore-arc lithosphere is illustrated in pink. Magma types

are Fore-arc Basalt (FAB) and Boninite (BON), divided into Basaltic Boninite (BSB), Low-Si Boninite (LSB) and High-Si boninite (HSB). DMM is Depleted MORB Mantle. Blue and red arrows refer to cold and hot slab input respectively. Black lines are schematic mantle vectors. A – the PAC-PPP boundary preceding subduction initiation; B – FAB-related crust is generated by sea-floor spreading beginning at about 51-52 Ma Ma; C – BSB and LSB crust is generated with further spreading accompanied by a robust fluid flux from the subducting Pacific plate; D – spreading wanes and HSB erupt at or before 48 Ma (cf. Ishizuka et al., 2006).

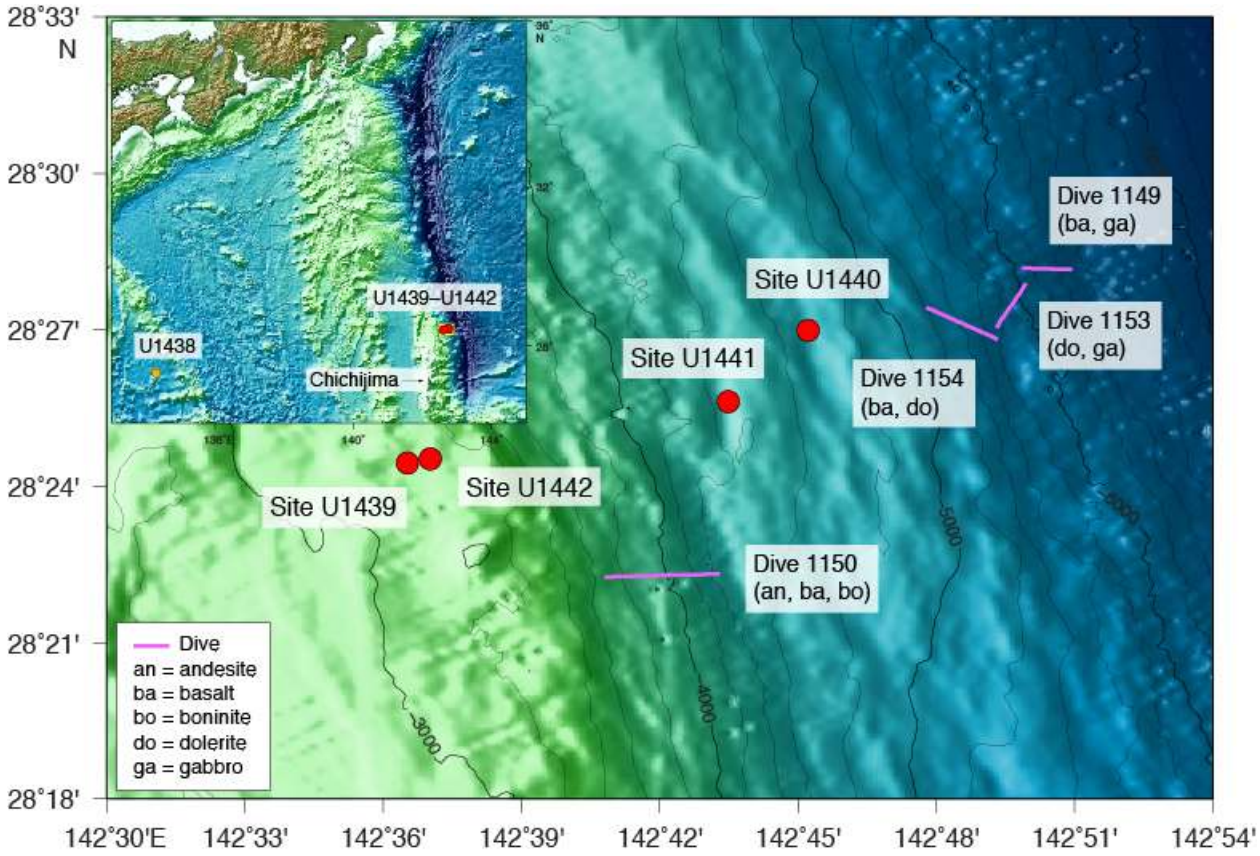
28°33' N
28°30'
28°27'
28°24'
28°21'
28°18'
142°30'E
142°33'
142°36'
142°39'
142°42'
142°45'
142°48'
142°51'
142°54'
U1439–U1442
U1438
Chichijima
Site U1439
Site U1442
Site U1441
Site U1440
Dive 1149 (ba, ga)
Dive 1153 (do, ga)
Dive 1154 (ba, do)
Dive 1150 (an, ba, bo)
Dive
an = andesite
ba = basalt
bo = boninite
do = dolerite
ga = gabbro
3000
4000
5000

Fig. 1

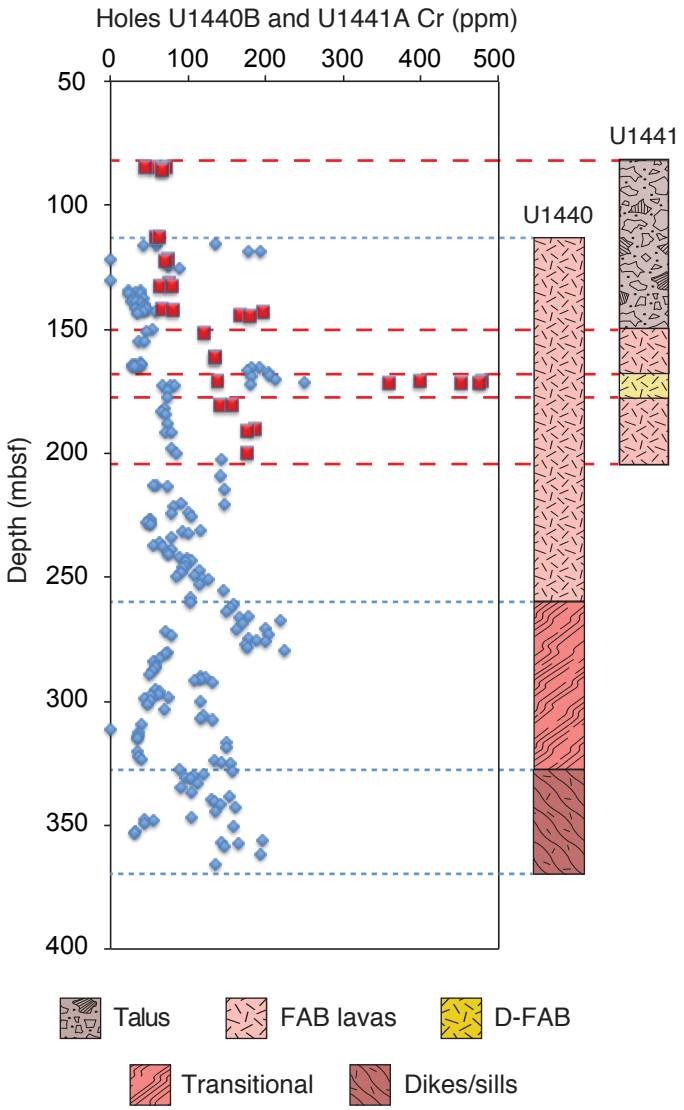
Holes U1440B and U1441A Cr (ppm)
0
100
200
300
400
500
50
100
150
200
250
300
350
400
Depth (mbsf)
U1441
U1440
Talus
FAB lavas
D-FAB
Transitional
Dikes/sills

Fig. 2

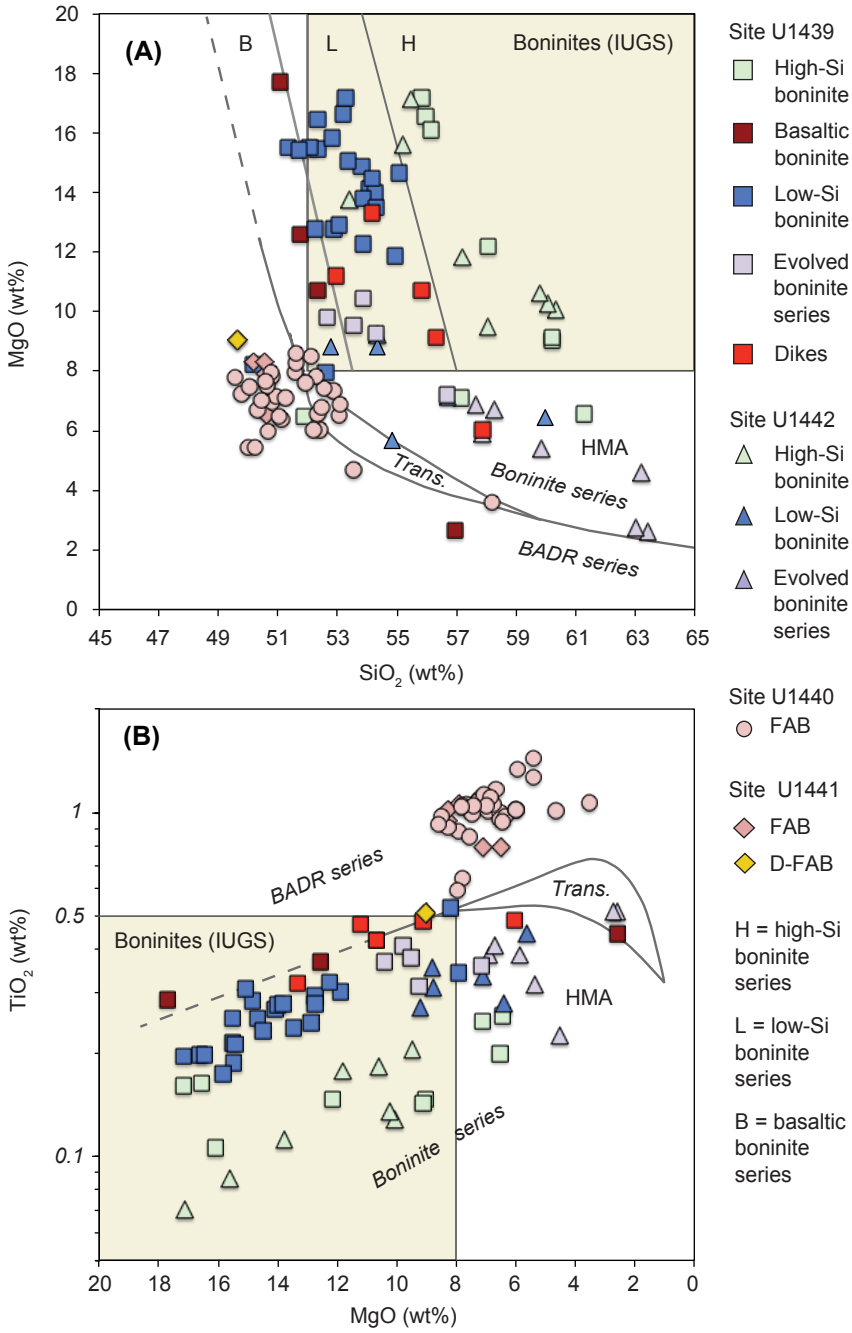
(A)
B
L
H
Boninites (IUGS)
HMA
Trans.
Boninite series
BADR series
MgO (wt%)
SiO2 (wt%)
Site U1439
High-Si boninite
Basaltic boninite
Low-Si boninite
Evolved boninite series
Dikes
Site U1442
High-Si boninite
Low-Si boninite
Evolved boninite series
(B)
BADR series
Trans.
Boninites (IUGS)
HMA
Boninite series
TiO2 (wt%)
MgO (wt%)
Site U1440
FAB
Site U1441
FAB
D-FAB
H = high-Si boninite series
L = low-Si boninite series
B = basaltic boninite series

Fig. 3

Fig. 4

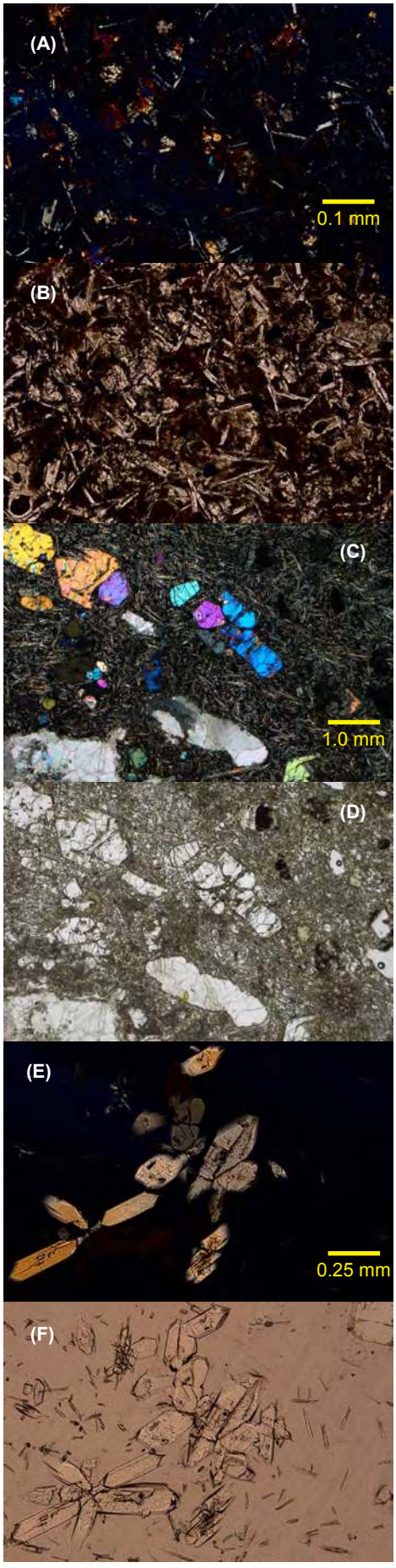

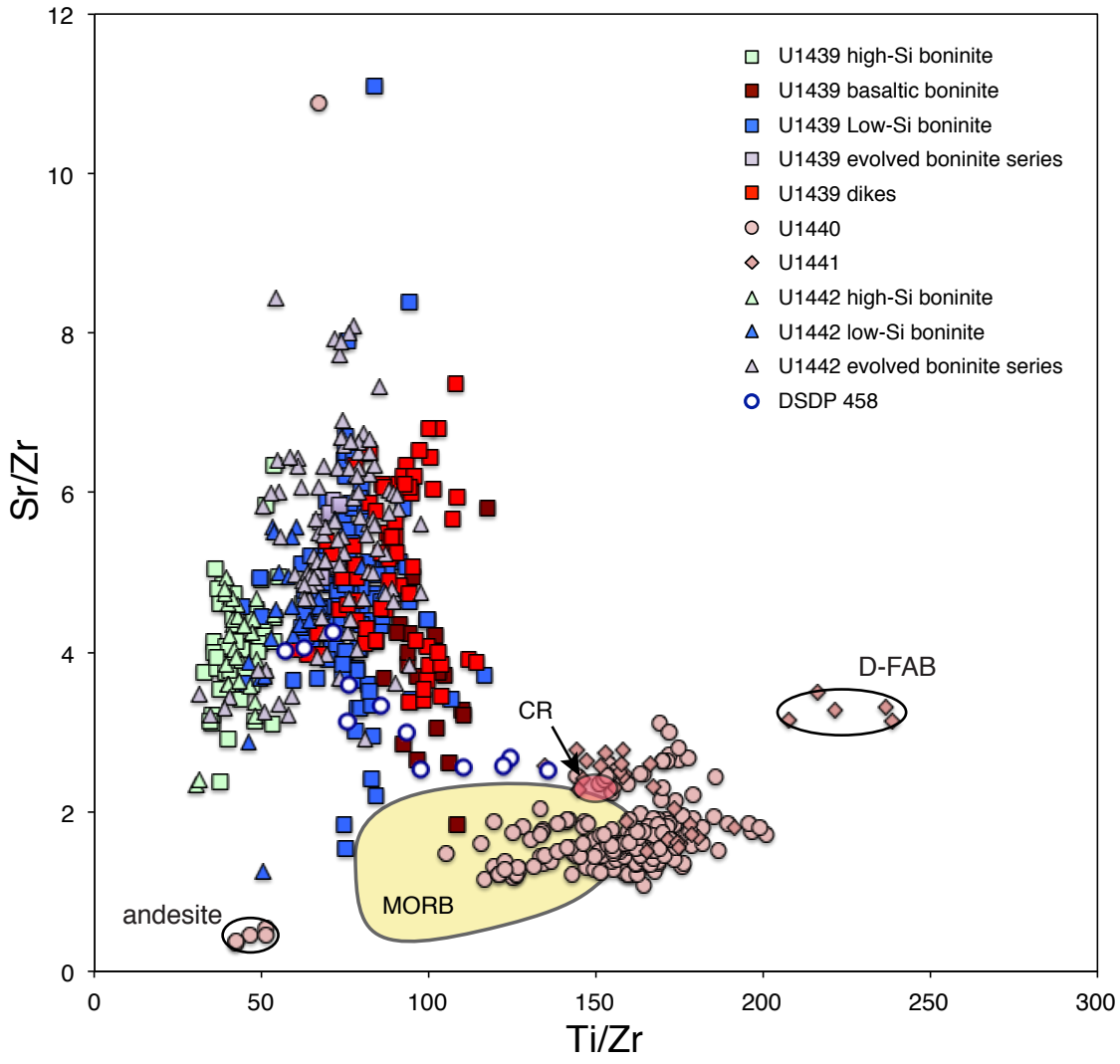
U1439 high-Si boninite
U1439 basaltic boninite
U1439 Low-Si boninite
U1439 evolved boninite series
U1439 dikes
U1440
U1441
U1442 high-Si boninite
U1442 low-Si boninite
U1442 evolved boninite series
DSDP 458
D-FAB
CR
MORB
andesite
Sr/Zr
Ti/Zr
0
2
4
6
8
10
12
0
50
100
150
200
250
300

Fig. 5

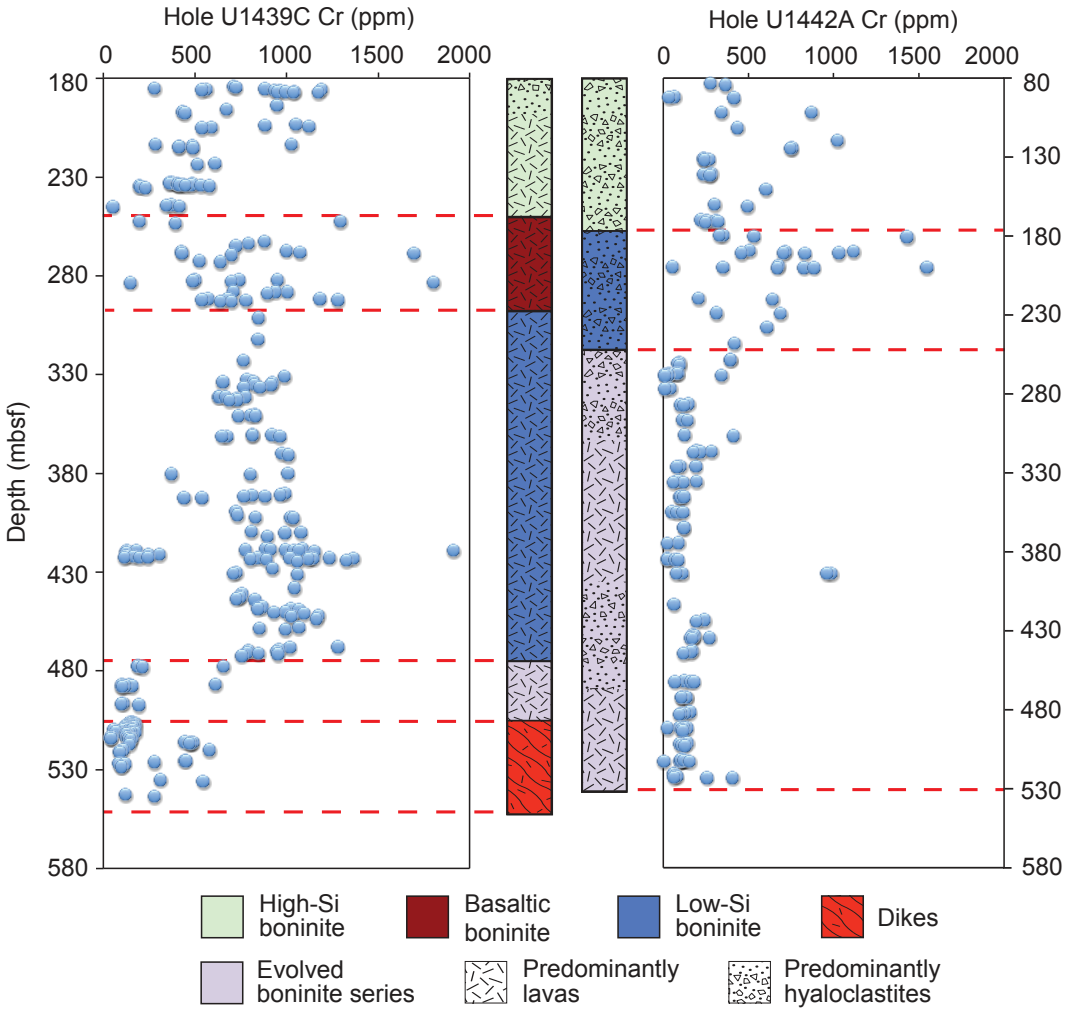
Hole U1439C Cr (ppm)
0
500
1000
1500
2000
Hole U1442A Cr (ppm)
0
500
1000
1500
2000
Depth (mbsf)
180
230
280
330
380
430
480
530
580
80
130
180
230
280
330
380
430
480
530
580
High-Si boninite
Basaltic boninite
Low-Si boninite
Dikes
Evolved boninite series
Predominantly lavas
Predominantly hyaloclastites

Fig. 6

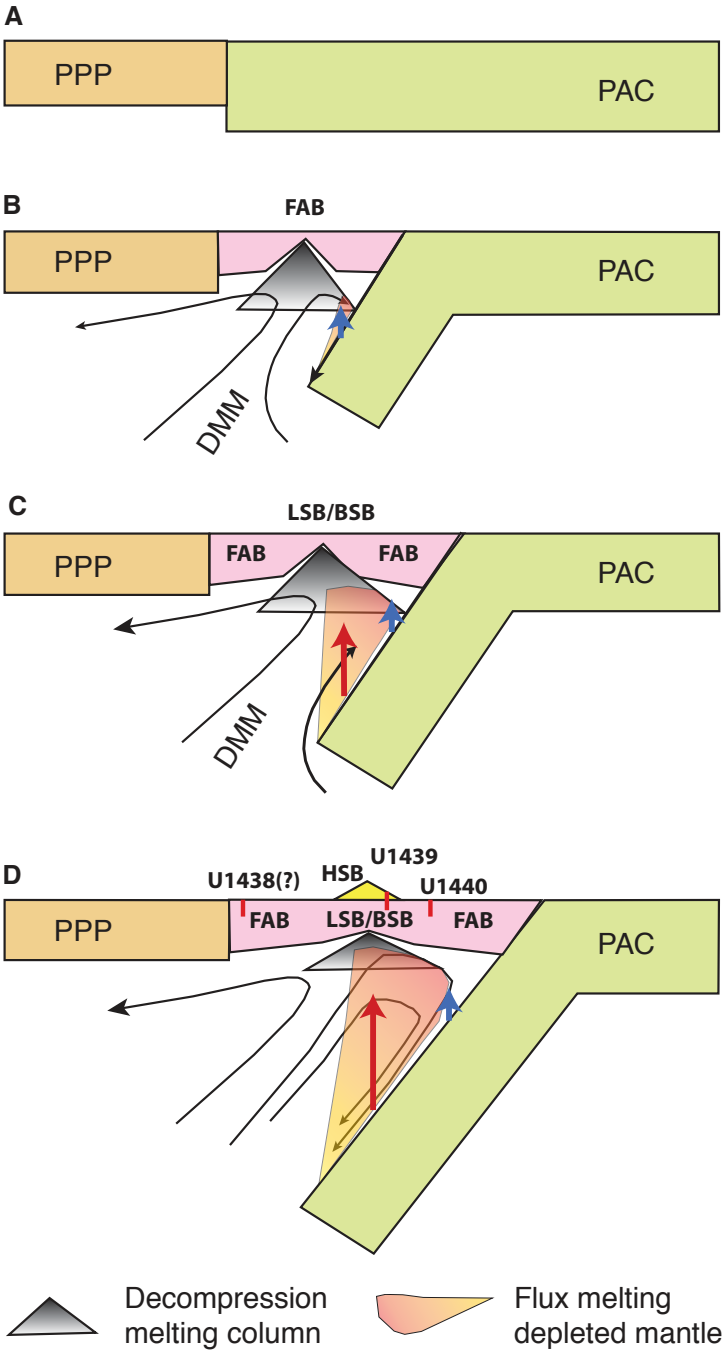
A
PPP
PAC
B
FAB
PPP
PAC
DMM
C
LSB/BSB
PPP
FAB
FAB
PAC
DMM
D
U1438(?)
HSB
U1439
U1440
PPP
FAB
LSB/BSB
FAB
PAC
Decompression melting column
Flux melting depleted mantle

Fig. 7